Measurement of ground motion in various sites

Wilhelm Bialowons, Ramila Amirikas, Alessandro Bertolini, and Dirk Krücker*
Deutsches Elektronen-Synchrotron DESY, 22603 Hamburg, Germany
(Dated: October 26, 2007)

Ground vibrations may affect low emittance beam transport in linear colliders, Free Electron Lasers (FEL) and synchrotron radiation facilities. This paper is an overview of a study program to measure ground vibrations in various sites which can be used for site characterization in relation to accelerator design. Commercial broadband seismometers have been used to measure ground vibrations and the resultant database is available to the scientific community. The methodology employed is to use the same equipment and data analysis tools for ease of comparison. This database of ground vibrations taken in 19 sites around the world is first of its kind.

I. INTRODUCTION

Ground motion may prove a limiting factor in the optimization of future accelerators. Beam stability becomes imperative in linear colliders and FELs where micron-sized beams will be accelerated. Ground motion and facility noise may cause vibration of the accelerating components, such as accelerating modules containing radio frequency cavities and magnets, which may lead to beam emittance growth. In the case of the International Linear Collider, ILC [1], an initially 500 GeV (center-of-mass) collider, e^+e^- beams, having a vertical dimension of ∼6 nm and ∼640 nm in the horizontal direction at the IP (Interaction Point), will be collided at a nominal peak luminosity of 2×10^{34} cm^2 s^{-1} for high energy particle research. Ensuring such minuscule beams maintain a high rate of head-on collision is a challenge and every effort should be undertaken to minimize possible causes of beam jitter. In addition, total length of the chosen ILC site will be ∼30 km in its initial phase before future upgrade to 1 TeV. The two main linear accelerating (linac) sections which will accelerate electron and positron beams, will comprise 2/3 of the total site length. A profound knowledge of ground vibrations of a site over such a long distance is also a point to consider in planning a linear accelerator. Moreover, preserving small bunch emittance over such a long distance can be challenging.

Another example for which ground vibrations may affect the beam stability is the European X-ray Free Electron Laser (XFEL) [2], now planned at DESY. The required beam offset tolerance in the undulators is 0.1σ, where σ is the root mean square (rms) of the beam size, in both horizontal and vertical directions within the straight trajectory through the 250 m long undulators. The beam size in the undulator is 30 μm and a 0.1σ offset tolerance is therefore, 3 μm [2]. In addition, the trajectory through the undulator has to be not only stable but absolutely straight by the same magnitude, i.e., 3 μm. Assuming uncorrelated quadrupole motion, the rms trajectory motion at the end of the undulators is a factor 10-15 higher than the rms of the quadrupole jitter, thus, leading to an upper limit of about 200 nm for the quadrupole motion [3]. Moreover, the pointing stability of the photon beam on a sample, 800 meters away in the experimental hall does impose stringent beam stability requirements due to possible beam jitter.

In the case of third generation synchrotron radiation facilities, such as PETRA III in DESY, stable beams at radiation source points are desired. Ground motion may cause positional instability, i.e., jitter, of the sample under study and emittance growth. If left uncorrected, it can reduce the efficiency of beam time for a particular experiment.

A site stability study in DESY was initiated to measure ground motion resulting from urbanization, the so called "cultural noise", dominant at f ≥ 1 Hz, and geology, spanning many high energy laboratories and synchrotron radiation

*The authors may be contacted via e-mail: wilhelm.bialowons@desy.de,ramila.amirikas@desy.de,alessandro.bertolini@desy.de, dirk.kruecker@desy.de

facilities around the world. This very first comprehensive database of ground vibrations, measured in 19 sites around the world, is available to the scientific community [4].

II. METHODOLOGY AND EQUIPMENT

To ensure a uniform site ground vibrations database, same equipment, measurement technique and analysis tools were employed throughout the site measurement program. This renders characterization of various sites feasible. Two sites in Germany, a former salt mine named Asse, in the state of Lower Saxony and a seismic station, named Moxa, near Jena, in the state of Thuringen, were chosen as reference sites. Both sites were measured in two consecutive years, 2003 and 2004, as a check of reproducibility of the results. Both of these sites are in a low "cultural noise" area and are in geologically stable regions. Moreover, in the case of Asse, measurements at both surface and at a depth of 900 m were pursued to characterize the difference between surface and depth.

Measurement of other sites was done in several locations in the vicinity of each site to check for differences of "cultural noise" in each location within a site. For instance, in a building, on a side road, inside an experimental area/control room and in more than one location inside accelerator tunnels. In most cases, measurement period consisted of weekdays and a weekend, to monitor the influence of day versus night and weekend vs. weekday in each site. Care was taken so that at least one full 24 hour measurement was obtained for each weekday and weekend so that there were no gaps in the measured hours. The measurements for this database took place within the 2003-2006 time scale.

The equipment used in this study consists of 5 state-of-the-art Güralp broadband triaxial seismometers, two CMG-6TD lightweight digital output seismometers (frequency response: 60 s-80 Hz) and three CMG-3TD (frequency response: 360(120) s-80 Hz) [5]. Each instrument is supplied with a Global Positioning System (GPS) antenna to synchronize their internal clock with satellite-based Coordinated Universal Time (UTC) during data acquisition anywhere in the world. A reformatting software converts UTC files into local time, i.e., Central European Time (CET). The internal hardware of the seismometers measures ground acceleration which is then internally integrated to obtain a voltage proportional to ground velocity. A 24-bit internal digitizer digitizes these signals (in three directions: horizontal, vertical and longitudinal) continuously during data acquisition. The data acquisition software is included in the same kit together with the seismometers by which one can control the sampling rate, the output file format and the duration of each measured file. All sites were measured with a sampling rate of 200 Hz, each file containing one minute seismic data in all three components. The self-noise of the instruments, integrated within the range $1 \leq$ f ≤ 80 Hz, is better than 0.02 nm [6].

III. DATA ANALYSIS

Here is a brief description of the analysis technique employed. For more information, please refer to [7]. For N discrete values measured in time T, the displacement Power Spectral Density (PSD) S_k of a noise signal is defined as

$$S_k = 2T\tilde{u}_k\tilde{u}_k^*, \tag{1}$$

if expressed in terms of the Fourier transform of ground displacement $\tilde{u}_k$. $k = fT$, an integer between 0 and $N/2$, is the normalized frequency and

$$S_k = 2T\frac{\tilde{\dot{u}}_k\tilde{\dot{u}}_k^*}{(2\pi k/T)^2}, \tag{2}$$

if expressed in terms of the Fourier transform of ground velocity $\tilde{\dot{u}}_k$. The factor two in Eqs. (2) and (1) appears because the values above the Nyquist frequency $f_N = f_s/2 = N/2T$ are mirrored due to the aliasing effect, i.e., $S_k = S_{N-k}$. In fact Eqs. (1) and (2) are equivalent. In these measurements, $f_s = 200$ Hz is the sampling rate and $T = 1$ minute. The relations above also take into account that the Fourier transform of the motion and velocity are related by

$$\tilde{u}_k = -i\frac{\tilde{\dot{u}}_k}{2\pi k/T}. \tag{3}$$

For N numbers $\dot{u}_n$, the discrete Fourier transformation is defined in general as

$$\tilde{\dot{u}}_k = \frac{1}{N}\sum_{n=0}^{N-1}\dot{u}_n e^{-ik\frac{2\pi}{N}n}, \tag{4}$$

and the reverse transformation is given by

$$\dot{u}_n = \sum_{k=0}^{N-1} \tilde{\dot{u}}_k e^{ik\frac{2\pi}{N}n}. \tag{5}$$

The rms of displacement, $\sqrt{\langle u^2 \rangle_l}$, above a cut-off frequency, normalized such that $f = l/T$, can be calculated from the power spectral density

$$\sqrt{\langle u^2 \rangle_l} = \sqrt{\frac{1}{T}\sum_{k=l}^{N/2} S_k}. \tag{6}$$

The PSD of displacement has a unit of $\mu\mathrm{m}^2/\mathrm{Hz}$. For better resolution of spectral details, the spectra are averaged over 15 minutes or even longer periods. Since "cultural noise" is dominant at f $\geq$ 1 Hz, in this work, the displacement PSDs measured were integrated at $1 \leq f \leq 80$ Hz, the upper limit matching the seismometer upper frequency response (see Sec. II).

The spectrum of correlation K_k of two synchronized signals $\tilde{u}_k$ and $\tilde{z}_k$, for any value k, is estimated by averaging over many 1 minute measurement data sets, is defined as

$$K_k = \frac{\langle \tilde{u}_k \tilde{z}_k^* \rangle}{\sqrt{\langle \tilde{u}_k \tilde{u}_k^* \rangle \langle \tilde{z}_k \tilde{z}_k^* \rangle}}. \tag{7}$$

K_k is a complex number by definition and coherence between two signals is hence defined as

$$C_k = |K_k|^2. \tag{8}$$

By definition, coherence of two signals is between 0 and 1.

IV. PSD SPECTRA OF GROUND MOTION

In this section, general features of PSD spectra of ground motion are illustrated by an example, taken from various sites in Germany. As the level of "cultural noise" differs with time, and depth, in a given site, it is informative to study the variation of "cultural noise" with time and depth. Besides the amplitude and spectral characteristics, spatial properties of the seismic waves, i.e., wavelength in general, are also necessary to evaluate the cumulative effect of the ground motion on the particle beam transport along the accelerator. These can be characterized by the correlation spectra.

A. Features of PSD spectra

Figure 1 shows the averaged vertical PSDs measured in the HERA tunnel in DESY (a shallow tunnel of several tens of meters in depth), two sites of the European XFEL, Osdorfer Born (labeled as XFEL Osdorf in the figure) where the XFEL electron linear accelerator will be positioned, Schenefeld (labeled as XFEL Schenefeld in the figure), where the beam distribution system and the experimental halls will be situated [2] and Ellerhoop (around 17 km north west of Hamburg) which was the designated IP region of the formerly proposed TESLA project [8]. The HERA tunnel and the future XFEL linear accelerator tunnel are/will be below the ground water table in quaternary sand. At the Schenefeld campus, the geology of the ground consists of marl, below the ground table level, formed by the last glacial period.

On the same plot, these spectra are compared with a reference site, seismic station Moxa. There are both common features and differences in these spectra, namely that in all, the microseismic peak from the sea waves $\sim 0.1 - 0.25$ Hz is seen. The shape of the spectra follows the $1/f^4$ random walk trend [9] and "cultural noise" which is detected at f $\geq$ 1 Hz, is a deviation of this trend (see Sec. V). The PSD of Moxa falls rapidly after the microseismic peak and at 1 Hz, its amplitude is lower by 3 orders of magnitude than HERA for example. The rms vertical displacement values, integrated at f $\geq$ 1 Hz, are summarized in Table III. The broad peak seen in the two XFEL sites around 10 Hz is caused by traffic. Incidentally, it is also seen in the HERA tunnel, albeit at a lower amplitude.

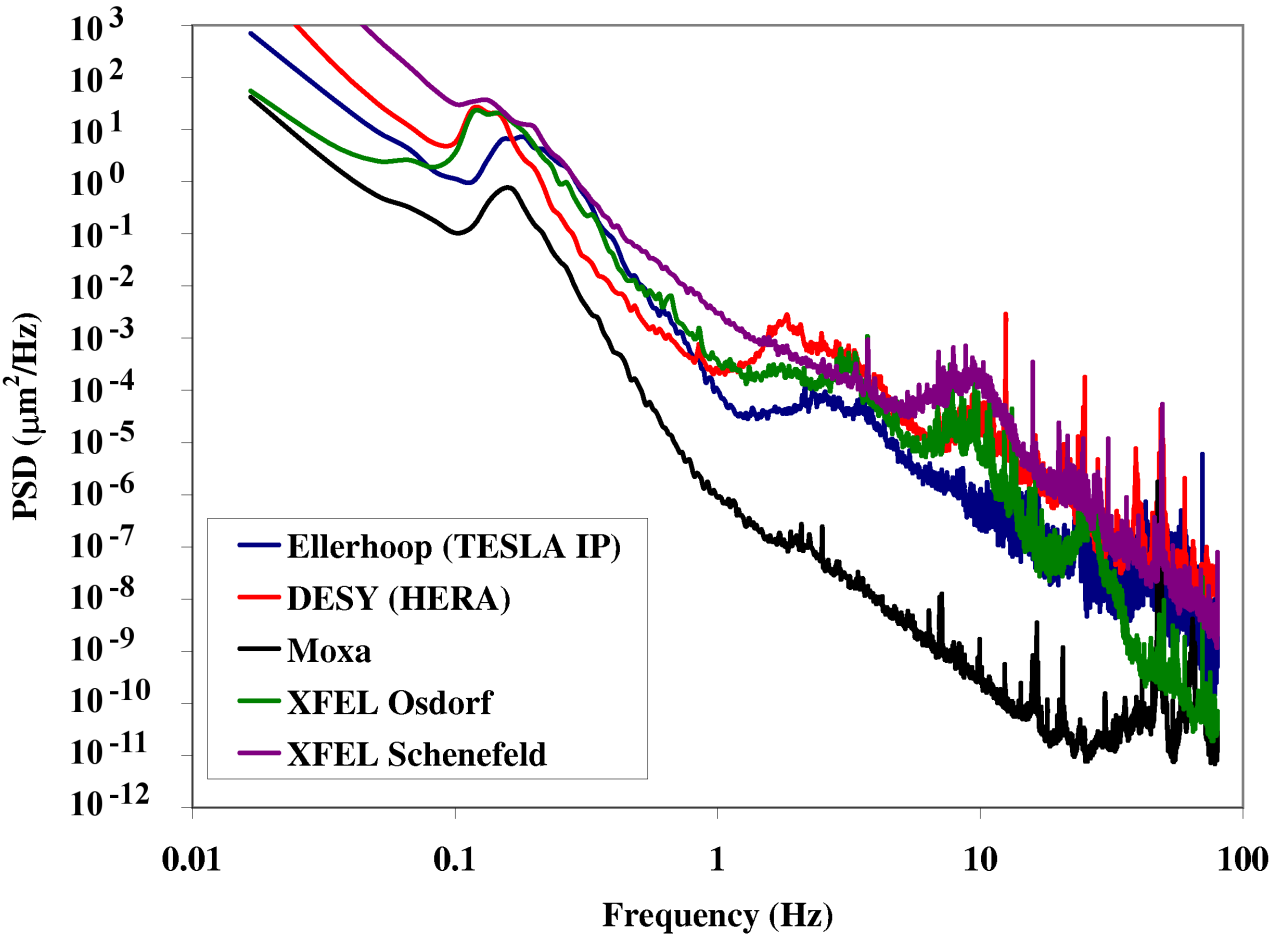

FIG. 1: (Color) Measured averaged vertical PSD spectra of various sites in DESY and vicinity as compared with a reference site, Moxa in Germany.

B. Variation of ground vibrations with time

Figure 2 shows variation in the vertical rms ground vibration with time for two measured sites: HERA tunnel, and Institute of High Energy Physics (IHEP) in Beijing, China, during the period of 24 April–2 May 2005. Variation of "cultural noise" is clearly observed during day/night time and weekend/weekday for the case of the HERA tunnel [6, 9]. A burst of activity is also seen on the first day of weekend (Saturday, 30 April 2005) in the afternoon. There are two aspects to note when comparing rms vibrations of HERA and IHEP: Firstly, IHEP has a much lower content of "cultural noise" than HERA by a factor of 4 and secondly, the variation between day/night and weekend/weekday is negligible. Amplitude rms versus time plots can provide information on instantaneous events, for example the passage of a heavy vehicle or train, and can be very useful in tracking possible sources of these events. These plots are available for every measured site in [4].

C. Ground vibrations in a tunnel

Depending on the rock geology, transfer of ground vibrations versus depth may differ from site to site. However, in general, the deeper a tunnel, the higher the attenuation of vibration sources from the surface. This is seen from the Figs. 3 and 4 where the PSDs of two laboratory sites are plotted at two depths: surface and ∼40 m deep in the case of Fermilab, as well as surface and the LHC tunnel (∼100 m deep) in the case of CERN [6]. Even though both of these sites have a rms vibration of a few tens of nanometers only, one can see the advantage of situating an accelerator in a tunnel rather than surface. On the same plots, Asse, a reference site in Germany (see Sec. II) has been plotted, highlighting again reduction of vibration sources in going from surface to a depth of 900 m.

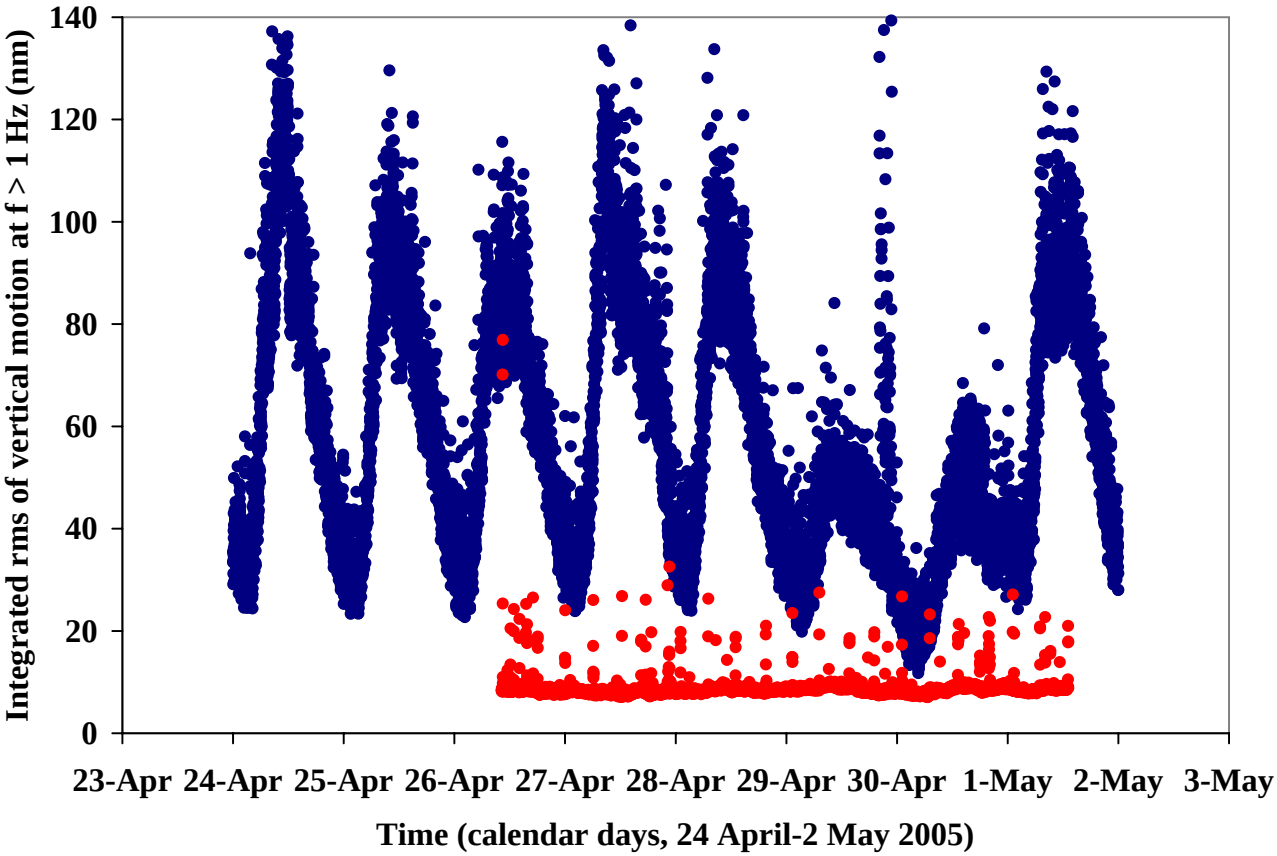

FIG. 2: (Color) Variation of vertical rms vibration of two sites, HERA tunnel in DESY (shown in dark blue) and IHEP in Beijing (shown in red), with respect to time.

It may be instructive to compare the difference, if any, between ground vibrations detected on the floor of a tunnel versus the ceiling. This comparison may be useful for example in the case of the XFEL for which it is proposed that the linac will be suspended from the tunnel ceiling [2]. To mimic such a tunnel layout, a measurement at the electron injection point in HERA was attempted. At this position, the floor of the transfer tunnel is directly above the HERA tunnel, i.e., acting effectively as the ceiling of the HERA tunnel. In a synchronized seismometer measurement, one seismometer was placed on the floor of the HERA tunnel and the other, on the ceiling. The distance between the two sensors was ∼5 m and the duration of data taking was three hours from 9:00 a.m. to 12:00 midday. Resultant PSDs together with the corresponding rms plots are shown in Fig. 5. At 1 Hz, the rms ratio between the floor and ceiling of the tunnel is at a few per cent level only. It is also interesting to note that at f $>$ 1 Hz, where technical noise can be detected in accelerator facilities, both sensors record a similar noise pattern up to f $\sim$ 15 Hz (see Sec. IV D below). This measurement illustrated that up to f $\geq$ 15 Hz, there is no difference in the ground vibrations experienced in either ceiling or floor of a tunnel. In this instance, dynamic stability of an accelerator, either suspended from the tunnel ceiling or placed on the floor, depends on the suspension/girder systems. However, long term stability of a tunnel ceiling depends on the tunnel construction.

D. Coherence spectra

Fig. 6 shows coherence spectra of two synchronized seismometers separated by various distances, in various locations at the DESY site, calculated using Eq. (7) in Sec. III. The measurements at 0 m, 10 m and 740 m (two experimental halls in the north-east and south-west directions of the PETRA ring) were performed inside buildings on the site, whereas, the measurement at 960 m was solely performed inside the HERA tunnel. The plot at 600 m was obtained from two synchronized seismometer measurements, one in the HERA tunnel and the other, in a building (surface measurement). Coherence plots are specific to each site. For the DESY site, one observes that there is good coherence,

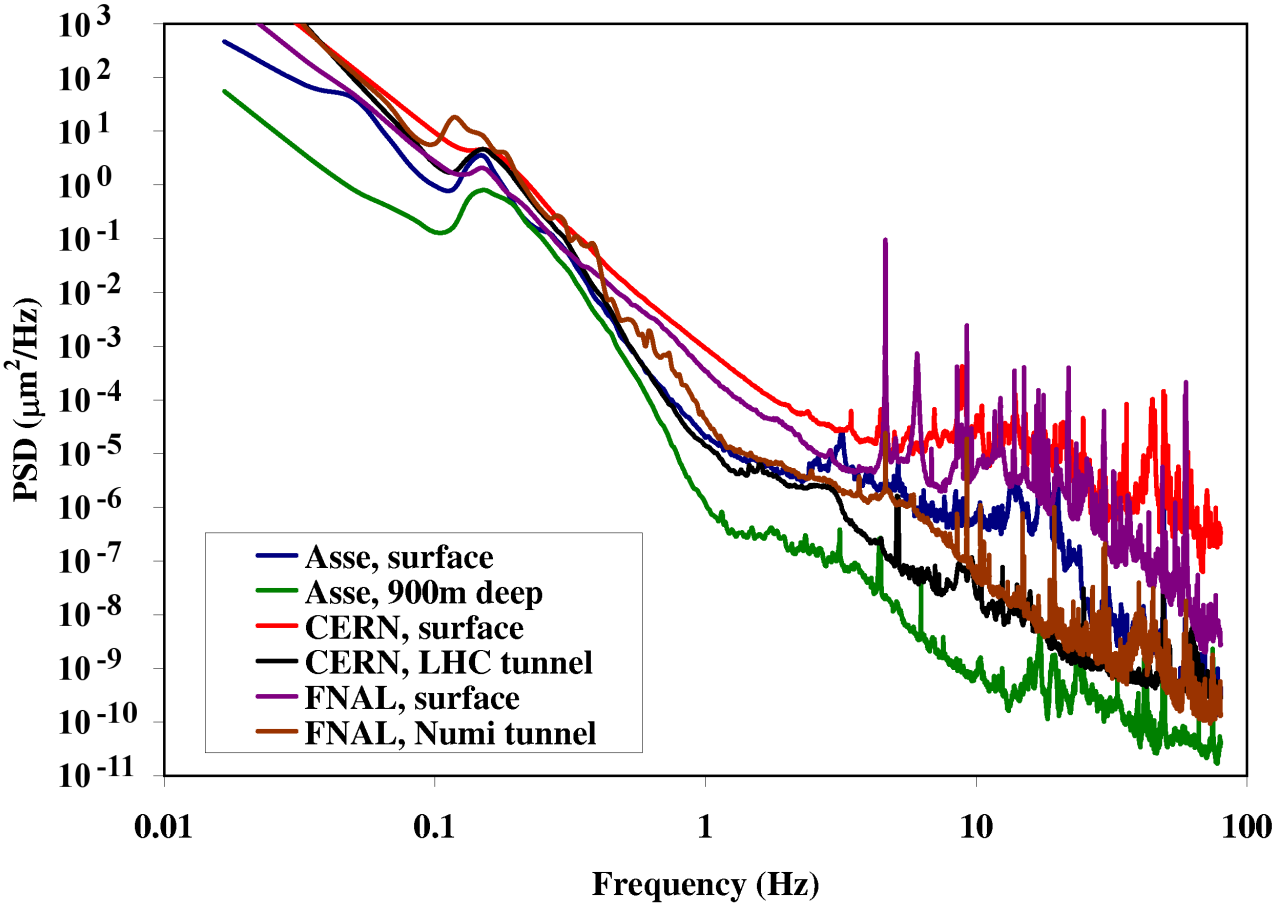

FIG. 3: (Color) Measurement of surface vs. depth (vertical) of average displacement PSDs of three sites: CERN, Fermilab and Asse.

i.e., $C_k > 0.9$, up to a frequency of ∼37 Hz at a small distance, ∼0 m. At a distance of 10 m, coherence drops markedly and C_k >0.9 up to 6 Hz only. It falls rapidly thereafter reaching a coherence of 0.5 at a frequency of 13 Hz and is zero at ∼16 Hz. This result manifests that the vibration of two points at a distance of 10 m is uncorrelated at f > 16 Hz. This is also observed in Fig. 5 where the vibration of the two seismometers, placed ∼10 m apart, is uncorrelated at f > 16 Hz. The dip observed in Fig. 6 at f < 1 Hz, may be caused by a low frequency, i.e., f < 1 Hz, signal which varies at the two points of detection induced by air flow or temperature variation when the sensors are not shielded from the environmental effects. As a consequence, a loss of coherence is seen in the signals detected by the seismometers at this frequency region. At distances larger than 0.5 km, the coherence at the DESY site is limited to the microseismic peak frequency only.

Usually, with good approximation, ground motion may be modeled as transverse waves which traverse isotropically along the connecting line of two seismic probes. In this model, the real part of the correlation equals to $J_0(2\pi fL/v)$, where J_0 is the zeroth order Bessel function, f is the frequency of the seismic waves, L is the distance between the two seismometers, and v is the wave phase velocity, which is frequency dependent [10]. The dispersive character arises from the dependence of the soil mechanical properties (modulus of elasticity, shear modulus, density etc.) on the depth. For example, in the case of Rayleigh waves, seismic waves penetrate the subsurface ground to a depth of approximately one/two wavelengths [11]. At low frequencies, the deepest, and generally the stiffest ground layers are involved in the seismic wave propagation, causing the phase velocity of the longer wavelength waves increase as well.

Similar data are available in literature for CERN [12] and Fermilab [13], while for the DESY site [14] were limited to short distance range. Simply by fitting the first zero of J_0, some representative values of the wave phase velocity can be extracted. This calculation was performed for the data shown in Fig. 6 and the results are displayed in Table I. With the same approach, using a much larger number of distance points and the whole domain of J_0, a velocity dispersion function was reconstructed for the SLAC site in the frequency range from 0.15 to 12 Hz [15].

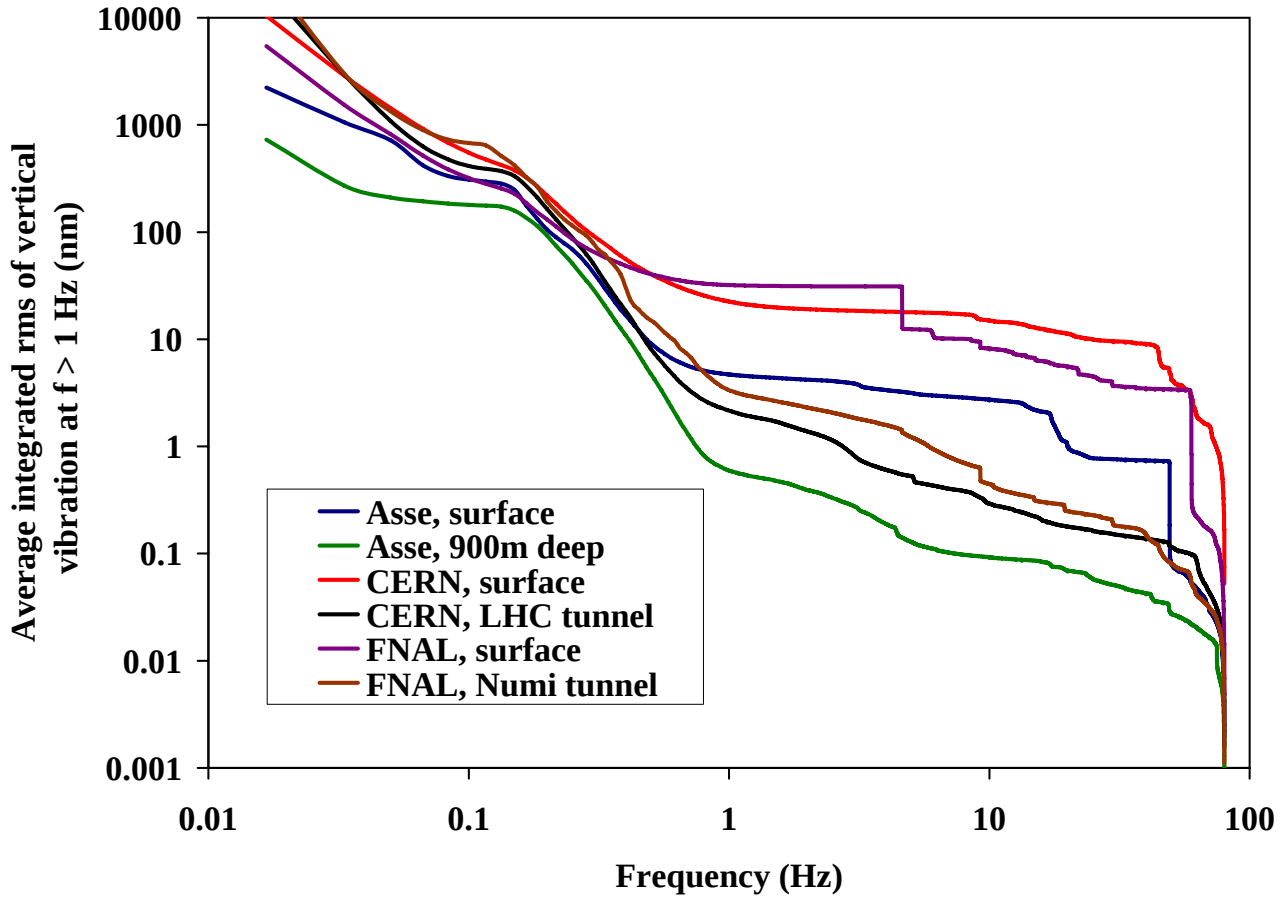

FIG. 4: (Color) Average integrated rms of the PSDs shown in Fig. 3.

TABLE I: Representative values of wave phase velocity measured at DESY. The frequency corresponds to the first zero of the zeroth order Bessel function.

distance (m)	frequency (Hz)	phase velocity (m/s)
10	16±0.5	420±10
600	0.81±0.02	1270±80
740	0.7±0.02	1360±80
960 [a]	0.65±0.05	1400±200

[a]Due to high level of measurement uncertainty at this distance, the error quoted is larger compared to the previous points.

E. Environmental effects

Objects move when responding to wind, and their motion is coupled with the ground. Wind acting on large objects such as trees and buildings, can produce movement in a very large frequency range. This movement can in turn be transferred to the ground which in turn can be superimposed to the "cultural noise" measured in a particular site.

As an example, in Fig. 7 results of a measurement done inside a building at DESY during different wind speeds are shown. Power spectra of vertical floor motion are binned by the mean wind speed and then averaged. Afterwards, the integrated rms has been computed. The effect of the wind activity on the seismic background inside the building looks systematic; the wind produces a broadband excitation, with amplitude and high frequency cut-off, increasing with the average wind speed. Table II shows the integrated rms measured in three representative frequency bands: 0.3-1.0 Hz, labeled as rms_1, 1.0-3.0 Hz, labeled as rms_2, and 3.0-10.0 Hz, labeled as rms_3, as a function of the average wind speed.

Generally, one can observe a strong power increase during the winter months and a shift of the microseismic peak to slightly longer periods. No significant diurnal effect is visible. These seasonal variations are due to the increase in

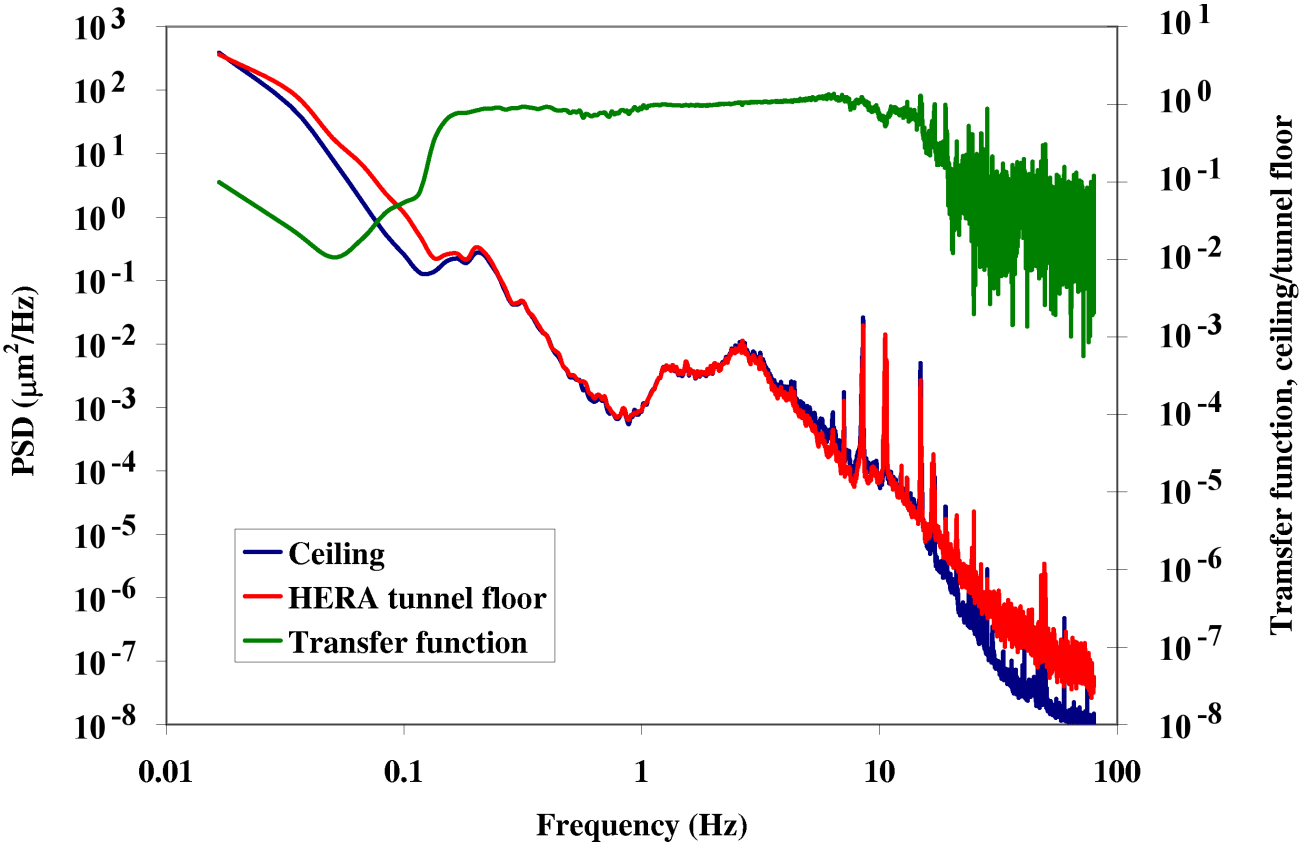

FIG. 5: (Color) Average vertical PSD and rms of HERA tunnel floor versus ceiling at the HERA electron injection point.

TABLE II: Integrated vertical rms measured in a building in DESY. The broadband nature of the wind effect is clearly shown by the enhancement of the rms amplitude in each of the three selected frequency bands.

Wind speed (m/s)	rms_1 (nm)	rms_2 (nm)	rms_3 (nm)
2	25	36	27
4	36	41	32
6	43	54	42

the intensity of Atlantic storms during the fall and winter for the particular case of DESY as shown in Fig. 8, where vertical PSD measured in weekends in three different seasons are compared.

V. SITE CHARACTERIZATION

Having a database of 19 measured sites enables one to characterize the "cultural noise" content of each site. One method is to divide the average displacement PSD spectra into several frequency bands and integrate to obtain average rms values for that band. In Figs. 9 and 10, the original PSD spectra were divided into 6 frequency bands of $f_{band} < f < 80$ Hz, where f_{band}= 0.1, 0.3, 1.0, 3.0, 10.0 and 30.0 Hz. The lines through the points are to aid the eye only. In these figures, the differences in the "cultural noise" content of different sites are clearly seen at $f_{band} \geq$ 1.0 Hz since the average rms spectra are simplified into 6 data points. For example, bands 3 and 4 can be used to get a quick glimpse of the "cultural noise" content of a particular site. In Fig. 9, the average rms is between 10 nm to slightly more than 100 nm, signifying high "cultural noise" content, whereas, in Fig. 10, the values are much lower, from a fraction of 1 nm to slightly more than 10 nm, signifying low "cultural noise" content.

As it was noted in Sec. IV A, the amplitude of the PSDs decreases with the fourth power of frequency. However, this is the ideal case and deviation from this behavior highlights "cultural noise" content of a site. If one assumes purely random forces acting on the seismic sensor, the Fourier transform of the force and thereby, the acceleration of

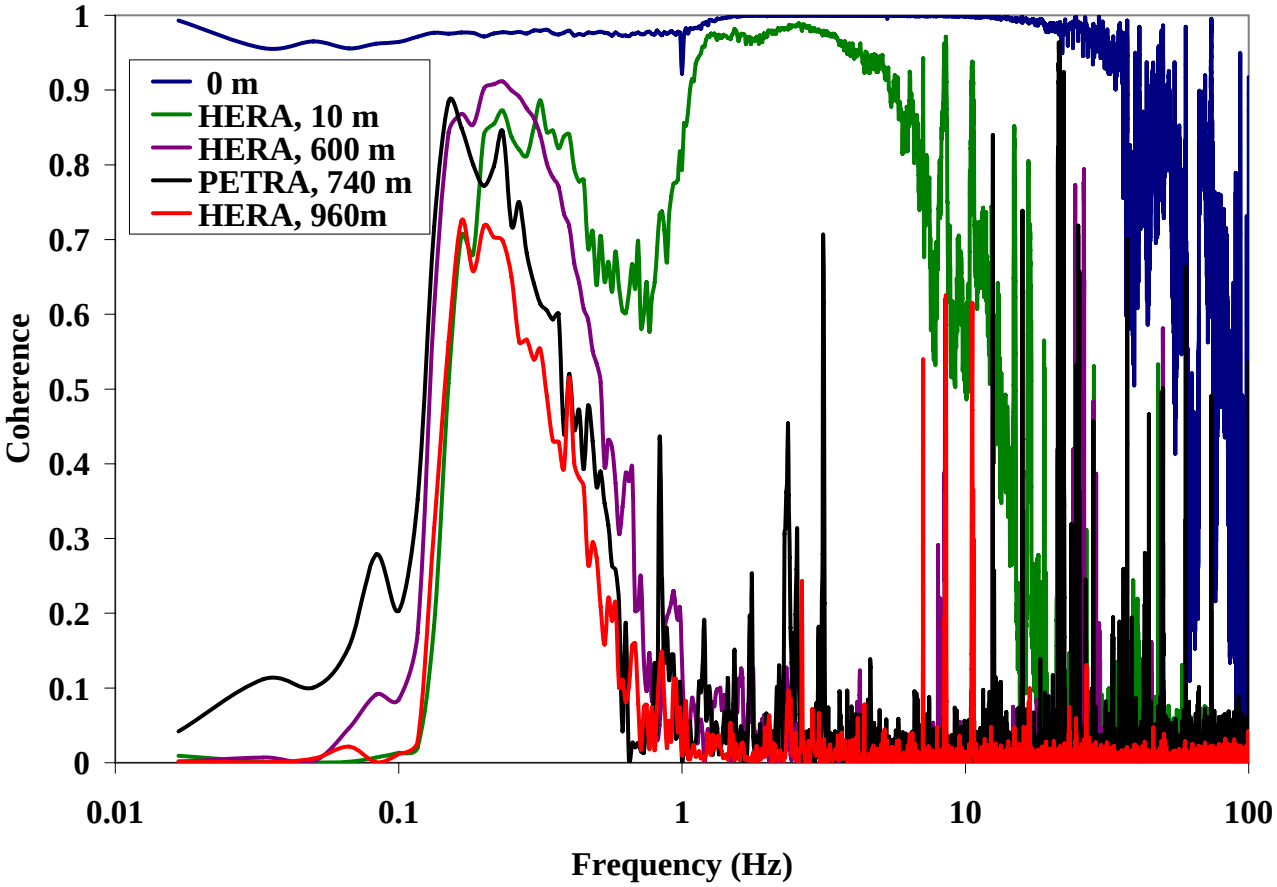

FIG. 6: (Color) Coherence spectra measured at different distances at DESY: 0 m, 10 m, 600 m, 740 m (diameter of PETRA ring) and 960 m in the HERA tunnel.

the seismic sensor will be a flat distribution up to the Nyquist frequency. Therefore, an efficient method to visualize the "cultural noise" content of a site, as a deviation from purely random noise, is to plot the acceleration amplitude spectral density $S_k^{(a)}$ in units of $\mu\mathrm{m/s}^2/\sqrt{Hz}$

$$\sqrt{S_k^{(a)}} = (2\pi k/T)^2\sqrt{S_k}. \tag{9}$$

Eq. (9) utilizes the relationship between the PSD of displacement and velocity, Sec. III Eqs. (1) and (2), and an analogous form of Eq. (3) in which the Fourier transform of displacement is written in terms of Fourier transform of acceleration

$$\tilde{u}_k = -\frac{\tilde{\ddot{u}}_k}{(2\pi k/T)^2}. \tag{10}$$

Results are shown in Figs. 11, 12 and 13. For simplicity of reference, they are classified into three groups: group A, group B and group C sites respectively.

Since measurements were taken with a constant sampling rate, discrete Fourier transform translates these equally spaced time bins into equally spaced frequency bins and since one plots with a logarithmic frequency scale, there would be many bins at higher frequencies where concurrently, the signal becomes noisier. Therefore the data in Figs. 11, 12 and 13 have been re-binned into logarithmic frequency bins. The microseismic peak is seen in all of these plots. However, group A sites show a clear deviation from the flat distribution expected as in the ideal case. Fig. 11 reveals the high "cultural noise" content of these sites confirming the conclusion reached earlier by looking at Fig. 9. Group A sites have an average rms value of more than 50 nm in general (see Table III). The site IHEP, Beijing, can be classified in group B, but is placed in Fig. 11 for comparison. Group B sites, Fig. 12, generally have an average rms vibration of 10-30 nm. Spring8, Harima in Japan which can be classified as group C, is shown together in Fig. 12

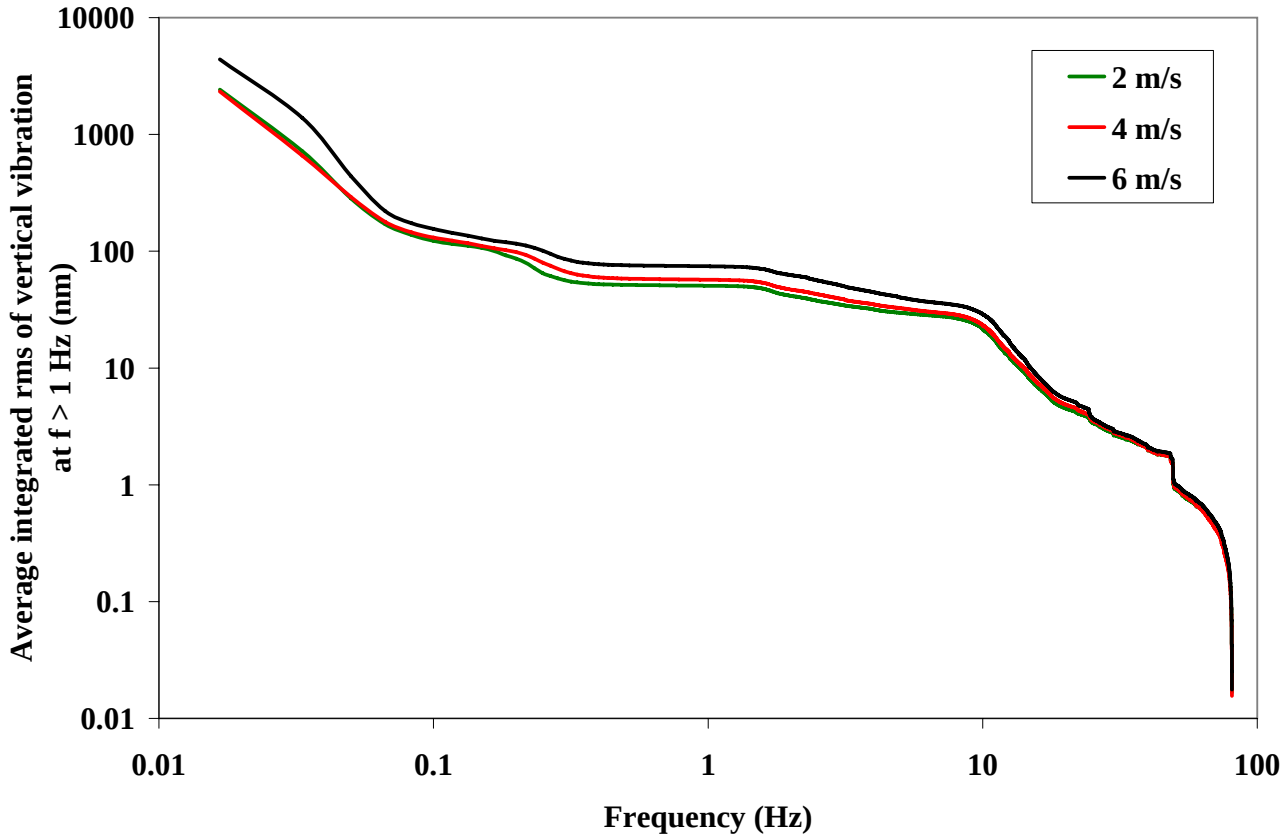

FIG. 7: (Color) Integrated rms displacement of a building floor (surface measurement), in the vertical direction, measured in DESY for three wind speeds during September 2006.

for comparison purposes only. Group C sites, Fig. 13, have an average rms vibration value of less than 10 nm. One can see that sites such as Asse and Moxa have a slight deviation from flat distribution due to detectable quantity of "cultural noise" even in these reference sites with low "cultural noise" content.

Table III is a summary of DESY's ground motion database in various sites, updated and revised compared to an earlier version [9]. The first two columns from the left are the average rms vertical vibration, in nm, and the spread σ in the rms values. The next two columns are selected one hour of highest and lowest rms vertical vibration values for each site. The motivation behind this calculation is to characterize a site by looking at its maximum and minimum rms vibration within a one hour period. The last two columns (far right) are the fitted mean of the calculated peak-to-peak (Pk-Pk) values and their corresponding Full Width at Half Maximum (FWHM) in nm. This calculation does not rely on Fourier transform of the raw signal and is therefore, another method to characterize a site on the basis of the instantaneous variation in the vibration sources. In this calculation, raw velocity signal of one minute data files was scanned to obtain maximum and minimum values in each one minute data file. Suitable bin width was used to histogram the results. One can observe that the Pk-Pk distributions are not normal, i.e., Pk-Pk $\neq 2\sqrt{2}$ rms. Deviation from this behavior is again characteristic to each site.

VI. SUMMARY

Ground vibrations should not be ignored in planning an accelerator facility. In this paper, ground vibrations measurement at 19 sites around the world were presented in view of the design of future accelerators. The objective of this study was to characterize these sites in accordance with the content of their "cultural noise". Analysis of the "cultural noise" in the measured sites showed that the sites in this database could be classified into three groups.

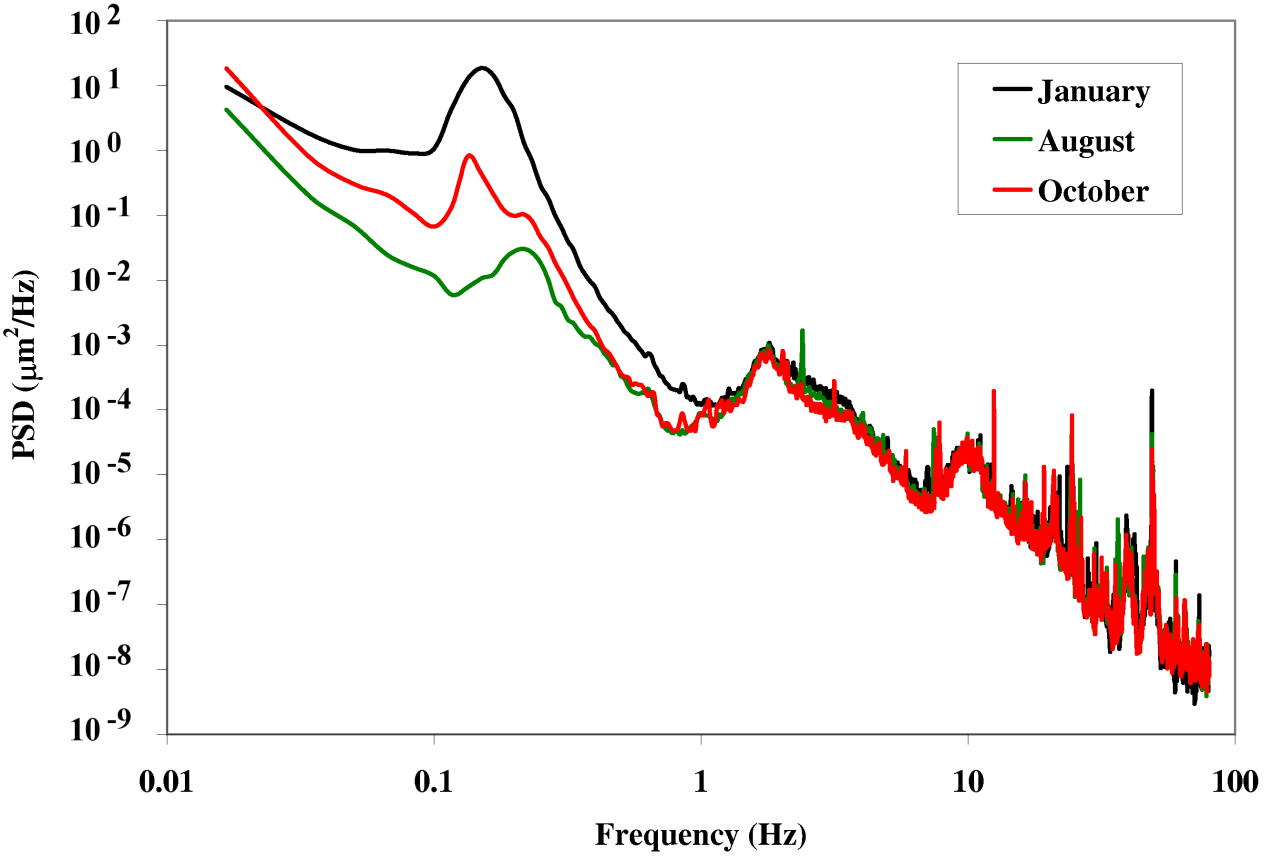

FIG. 8: (Color) Vertical PSD measured in the HERA tunnel within three different periods of the year. The amplitude of the microseismic peak shows changes by factors up to ∼30 between winter and summer.

ACKNOWLEDGMENTS

The authors would like to acknowledge Heiko Ehrlichmann for his contribution to the measurements of ground motion, and the persons who have provided hardware/software support, in particular, Carsten Kluth, Markus Kubczigk and Bartosz Poljancewicz. The authors are indebted to the assistance of numerous persons in all the sites visited. This work is in part supported by the Commission of the European Communities under the 6th Framework Program 'Structuring the European Research Area', contract number RIDS-011899.

[1] International Linear Collider (ILC) reference design report, draft released on 7 February 2007.
[2] XFEL Technical Design Report, http://www.xfel.net, edited by M. Altarelli et al., July 2006.
[3] W. Decking (private communication).
[4] <http://vibration.desy.de/> .
[5] Güralp Systems Ltd, <http://www.guralp.net/> .
[6] W. Bialowons, R. Amirikas, A. Bertolini, D. Kruecker, *Proceedings of the 10th Biennial European Particle Accelerator Conference* (Edinburgh, UK, 2006), Report No. EUROTeV-Report-2006-033.
[7] W. H. Press, B. P. Flannery, S. A. Teukolsky and W. T. Vetterling, *Numerical Recipes, The Art of Scientific Computing* (Cambridge University Press, Cambridge, 1986).
[8] TESLA, Tera-Electronvolt Superconducting Linear Accelerator, Technical Design Report, Part II, The Accelerator, edited by R. Brinkmann et al., Deutsches Elektronen Synchrotron, Hamburg (DESY), March 2001.
[9] R. Amirikas, A. Bertolini, W. Bialowons, H. Ehrlichmann, *Proceedings of NANOBEAM2005, 36th ICFA Advanced Beam Dynamics Workshop,* edited by Y. Honda, T. Tauchi, J. Urakawa, Y. Iwashita and A. Noda, p. 202; Report No. EUROTeV-Report-2005-023.
[10] Andrey Sery and Olivier Napoly, Phys. Rev. E**53**, pp. 5323-5337 (1996).

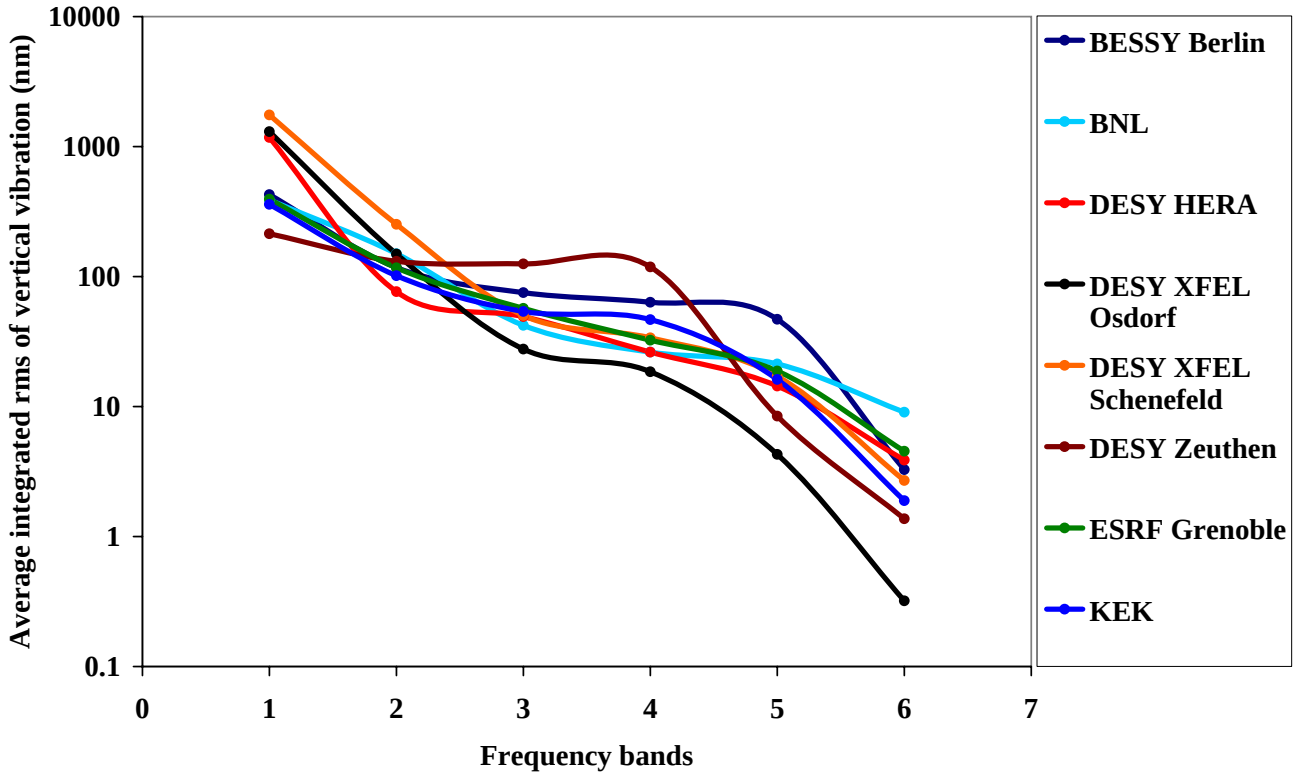

FIG. 9: (Color) Average rms in 6 frequency bands, as described in the text, of several measured sites with high "cultural noise" content.

TABLE III: DESY's database of ground motion, measured in 19 sites, is summarized in this table. The meaning of each column has been explained in the text.

Site location	Average rms (nm)	σ (nm)	Highest rms (nm)	Lowest rms (nm)	Pk-Pk (nm)	FWHM (nm)
ALBA, Barcelona, Spain	18.8	9.5	42.0	9.1	86.6	122.0
APS, Argonne, U.S.A.	10.7	1.0	11.0	9.8	68.5	57.7
Asse, Germany (salt mine)	0.6	0.1	0.7	0.5	13.1	35.4
BESSY, Berlin, Germany	75.0	28.1	140.7	53.1	249.3	158.4
BNL, Upton, U.S.A.	89.6	30.2	135.3	29.1	383.6	558.2
CERN, Geneva, Switzerland[a]	1.9	0.8	2.8	0.9	21.6	54.1
DESY HERA, Hamburg, Germany	53.3	18.9	77.0	34.8	178.4	204.3
DESY XFEL, Osdorf, Germany	29.1	11.9	48.4	19.5	147.9	196.9
DESY XFEL, Schenefeld, Germany	41.1	16.6	70.0	35.1	179.6	245.3
DESY, Zeuthen, Germany	64.4	40.4	75.6	88.5	115.3	240.0
Ellerhoop, Germany[b]	18.2	8.4	35.9	9.3	102.0	162.4
ESRF, Grenoble, France	74.0	34.9	137.2	40.2	163.3	179.8
Fermilab (FNAL), Batavia, U.S.A.[c]	3.0	0.9	4.0	2.2	24.4	49.1
IHEP, Beijing, China	8.5	0.5	9.0	8.1	49.5	18.6
KEK, Tsukuba, Japan	80.5	36.0	125.1	38.0	228.4	277.0
LAPP, Annecy, France[d]	3.6	1.6	7.0	1.9	35.7	66.3
Moxa, Germany (seismic station)	0.6	0.1	0.9	0.5	7.9	16.8
SLAC, Menlo Park, U.S.A.[e]	4.9	1.2	7.4	4.1	61.4	117.9
Spring-8, Harima, Japan	2.0	0.4	2.5	1.8	22.4	40.3

[a]Numbers are for the LHC tunnel.
[b]TESLA (IP) [8]
[c]Numbers are for the Numi tunnel.
[d]Laboratoire d'Annecy-le-Vieux de Physique des Particules.
[e]Ground vibrations measurement at SLAC is limited to 20 Hz in frequency range unlike the rest of the database where the measurements are up to 80 Hz.

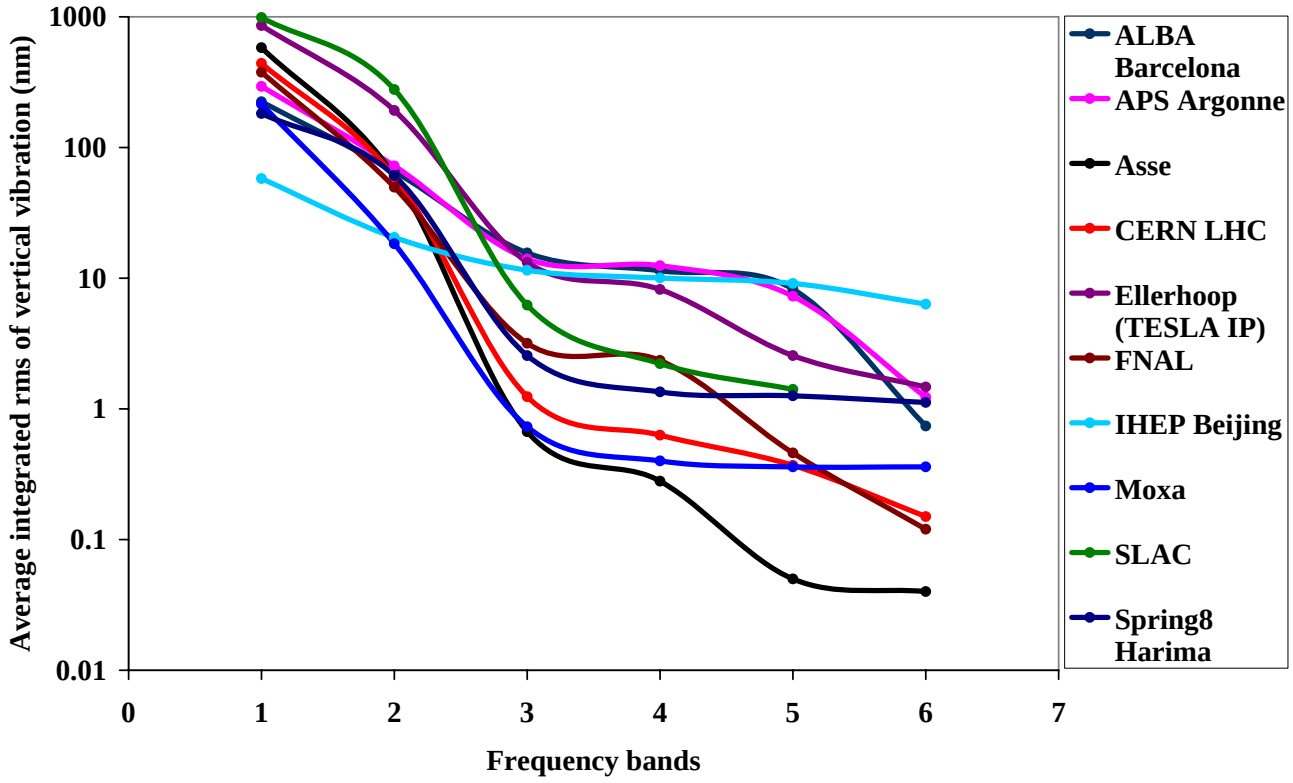

FIG. 10: (Color) Average rms in 6 frequency bands of several measured sites with lower "cultural noise" content than in Fig. 9.

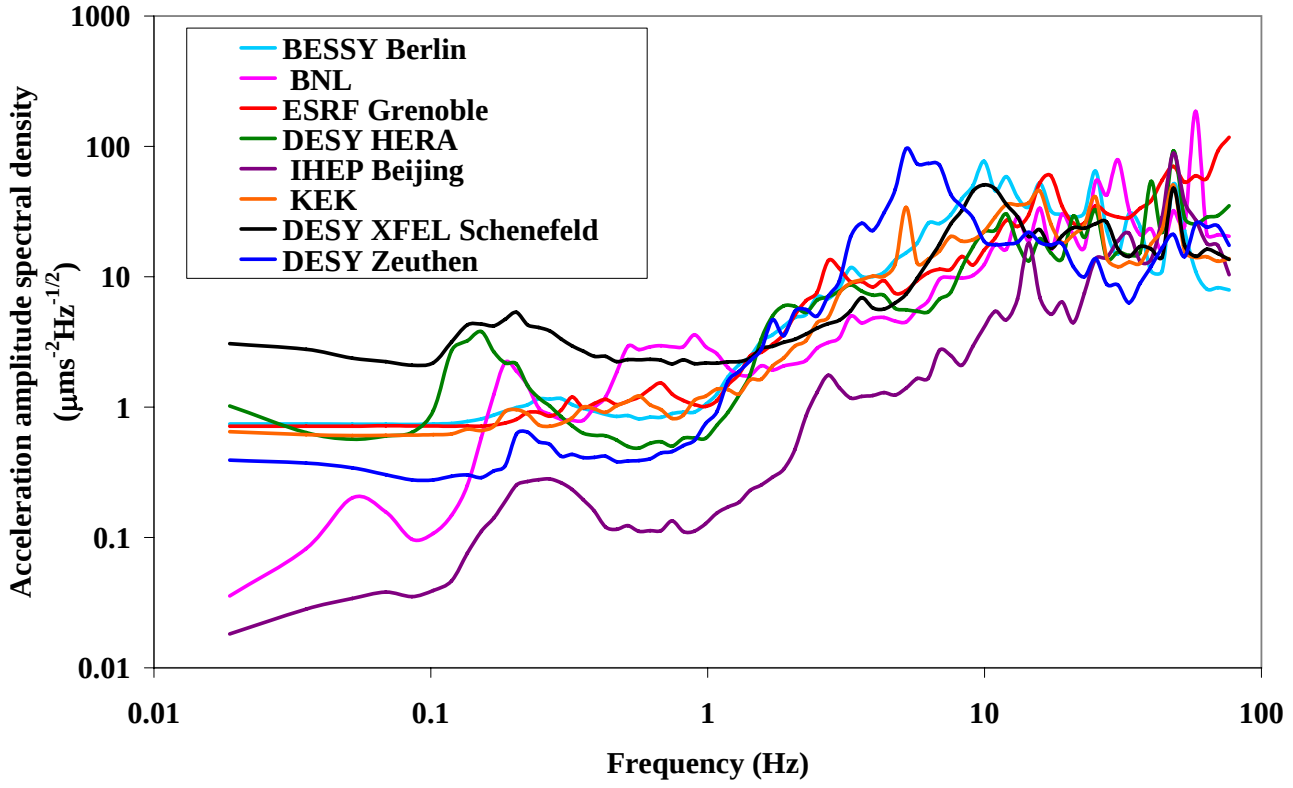

FIG. 11: (Color) Acceleration amplitude spectral density in units of $\mu\mathrm{m/s}^2/\sqrt{Hz}$ per frequency bin is plotted to characterize group A sites.

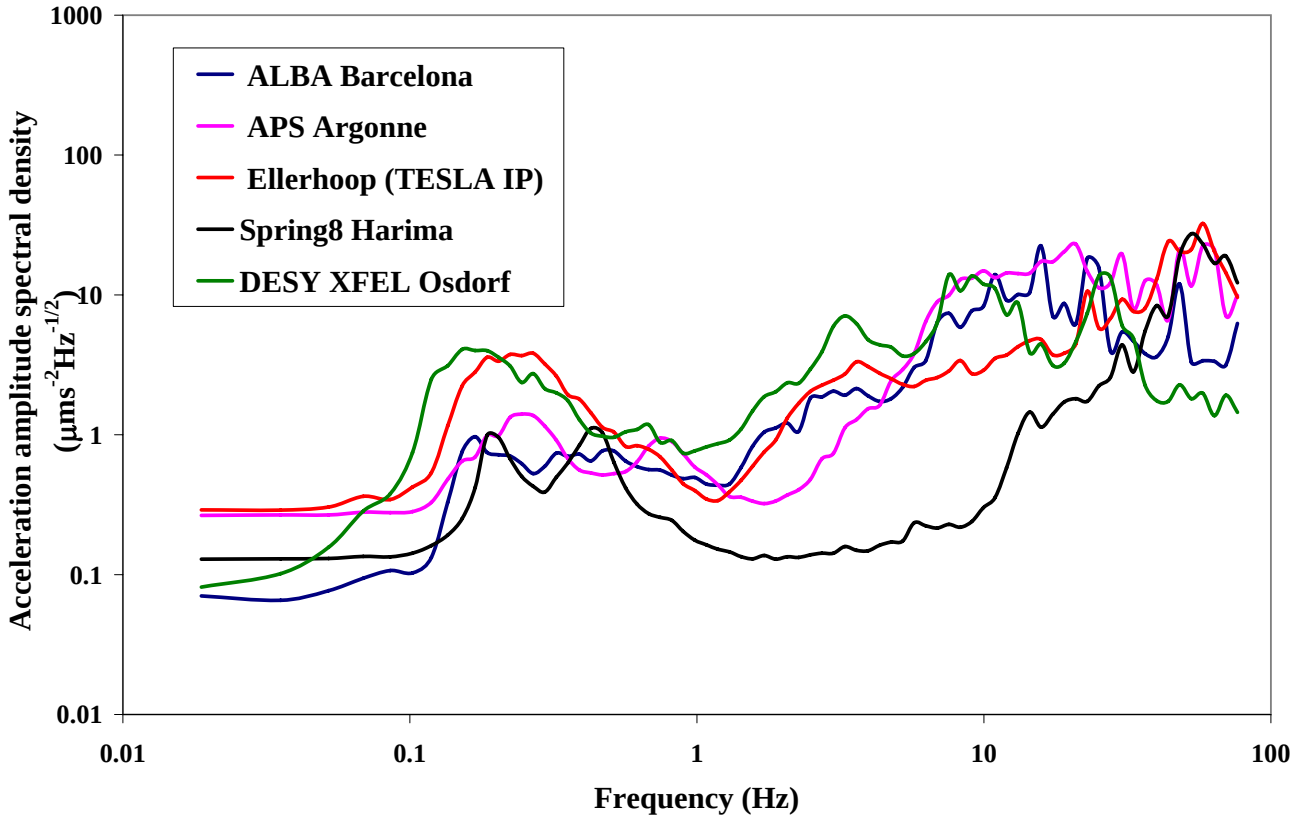

FIG. 12: (Color) Same plot as Fig. 11 for group B sites.

[11] K. Aki and P. G. Richards, *Quantitative Seismology, 2nd Edition* (University Science Books, Herndon, USA, 2002).
[12] V. M. Juravlev, A. A. Sery, A. I. Sleptsov, W. Coosemans, G. Ramseier and I. Wilson, Report No. CERN-SL/93-53, 1993; Report No. CLIC Note 217, 1993 (unpublished).
[13] B. Baklakov, T. Bolshakov, A. Chupyra, A. Erokhin, P. Lebedev, V. Parkhomchuk, S. Singatulin, J. Lach, V. Shiltsev Phys. Rev. ST Accel. Beams **1**, 031001 (1998).
[14] V. Shiltsev, B. Baklakov, P. Lebedev, C. Montag, J. Rossbach, Report No. DESY-HERA Report 95-06,1995 (unpublished).
[15] NLC Zeroth-Order Design report, Appendix C, 1996.

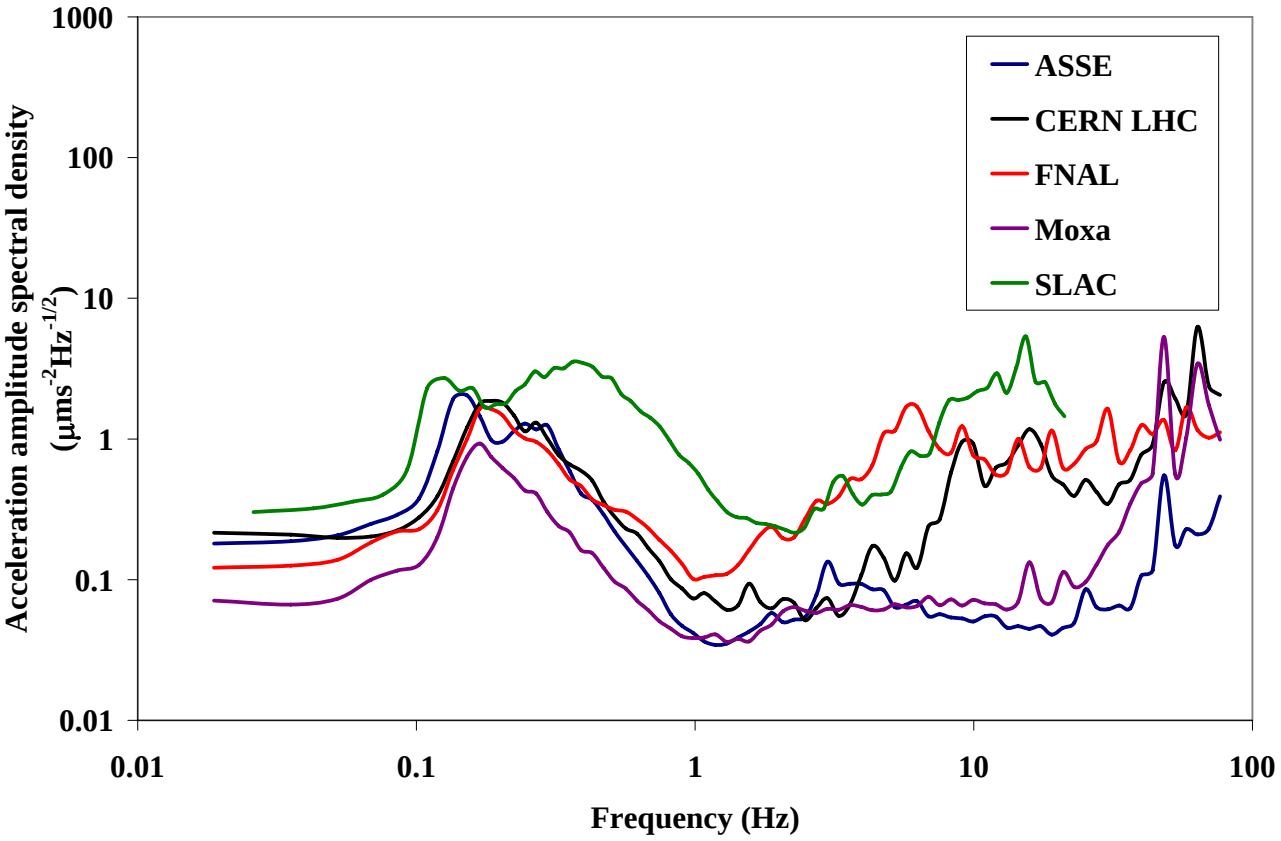

FIG. 13: (Color) Same plot as Fig. 11 for group C sites.